X-645-73-364

PREPRINT

NASA TM X- 70534

FIELD ALIGNED CURRENT OBSERVATIONS IN THE POLAR CUSP IONOSPHERE

B. G. LEDLEY

W. H. FARTHING

NOVEMBER 1973

GSFC — GODDARD SPACE FLIGHT CENTER —

GREENBELT, MARYLAND

Field Aligned Current Observations in the Polar Cusp Ionosphere

B. G. Ledley and W. H. Farthing

NASA Goddard Space Flight Center
Greenbelt, Maryland 20771

November 1973

(Submitted for publication in Journal of Geophysical Research)

ABSTRACT

Vector magnetic field measurements made during a sounding rocket flight in the polar cusp ionosphere show field fluctuations in the lower F-region which are interpreted as being caused by the payload's passage through a structured field aligned current system. The field aligned currents have a characteristic horizontal scale size of one kilometer. Analysis of one large field fluctuation gives a current density of 10^{-4} amp-m^{-2}.

Introduction

This paper presents an analysis of vector magnetic field measurements made on a sounding rocket flight in the Northern polar cusp region.

The polar cusps have been identified by low altitude satellite observations as dayside high latitude regions of intense precipitation of soft electrons and protons (Sharp and Johnson 1968, Burch 1968, Hoffman 1969, Heikkila and Winningham 1971). Low altitude satellite observations have also shown that these are regions in which, in common with all the auroral oval, large transverse magnetic field changes (Zmuda et al 1966, Zmuda et al 1970, Armstrong 1973, Berko et al 1973) and electric field fluctuations are detected (Heppner 1969, Maynard and Heppner 1970, Gurnett 1970). Both the magnetic and electric field variations have been interpreted as being primarily caused by movement of the satellites through spatial features rather than being primarily temporal effects.

High altitude satellite observations have extended the mapping of the polar cusp region to geocentric distances of ten earth radii, (Frank 1971, Russell 1971, Fairfield and Ness 1972) and have given further experimental support to the suggestions (Piddington 1965) that the cusp is a region to which magnetosheath plasma has direct access.

There have, however, been very few observations in this region of the ionosphere below 400 km. The only magnetic field measurements are those by Cahill (1959), who reported the detection and measurement of a horizontal sheet current during a sounding rocket flight, and by

Choy et. al. (1971) who reported the possible observation of a very intense horizontal current filament at 105 km. during a sounding rocket flight.

Two Nike Tomahawk rockets, 18.128 and 18.129 were flown from Hall Beach, (the Fox-Main Dewline station) Northwest Territories, Canada on March 22nd and March 19th 1971 respectively. Their payloads, to be described below, were identical and were designed to make vector magnetic field measurements. In the same expedition, but on different days, two other instrumented rockets, 18.126 and 18.127 were flown (Maynard and Johnstone 1973) to measure electric fields and low energy precipitating particles; reference will be made below to their results.

This paper presents the results of the 18.128 flight, which was in the polar cusp. Some of the 18.129 data will be shown here also, because that flight took place in relatively undisturbed magnetic fields and its data establishes qualitatively the noise level for our measurement and analysis technique.

Flight Conditions

Hall Beach is located at 79.73°N dipole latitude and 23.81°W dipole longitude (68.76°N geographic latitude and 81.22°W geographic longitude.) The 18.128 flight occurred at 10.6 hours magnetic local time (1650 UT). No radar tracking was used; the apogee time and altitude (265 km) were determined by comparison of the measurements with POGO(8/71) magnetic field model (Langel, 1973). A free fall motion including the Coriolis force was then used to describe the trajectory. The flight azimuth

and horizontal velocity were determined by comparison of the measured field vector throughout the flight with that obtained from the field model and the assumed trajectory. Values of horizontal velocity and azimuth determined in this way differed from nominal vehicle performance by an amount that could be accounted for by a 15° change in the launch azimuth. A horizontal velocity magnitude of .46 km/sec and an azimuth at apogee of 289° geomagnetic (305° geographic) were obtained. The flight plan path is shown dotted in Figure 1, in coordinates of dipole latitude and magnetic local time.

Figure 1 also shows the magnetic field disturbance vectors for the time of the flight. The vectors show the horizontal disturbance. The vertical disturbance in gammas (negative upward, 1 gamma (γ) = 1 nanotesla (nT)) is shown beside each vector. These were obtained from observatory magnetograms and from the records of the temporary field stations set up at Hall Beach and at CAM-4, another DEWline station located some 300 kilometers west of Hall Beach. To obtain observatory base lines from which to compute the disturbance field, field levels for the quietest days in 1970 and 1971 were interpolated to the flight date. For the temporary stations, the disturbances were referenced to the average field levels between 0200 UT and 0600 UT on March 21st, the day before the flight. This interval of time was exceptionally quiet at the temporary stations and also at many of the permanent high latitude observatories.

The disturbance pattern shown in Figure 1 is, in general, typical

of high latitude observations at low Kp values in a toward sector of the interplanetary field (Langel, private communication, 1973) although the negative vertical component at Godhavn is somewhat large relative to the magnitude of the horizontal components. It is apparent that the horizontal disturbance vectors for both Hall Beach and CAM-4 are large; this indicates the presence of localized ionospheric currents.

Reasons for expecting that the polar cusp was at this relatively high latitude at the time of the flight are the following: (1) the three hourly Kp value was 0+ and the values for the three preceding three-hourly intervals were 0^+, 0 and 1^-, and (2) the interplanetary magnetic field measured by IMP-6, which was at a geocentric distance of twenty earth radii, had a solar ecliptic azimuthal angle of between 270 and 315° for several hours preceding and for the hour following the flight (D. Fairfield, private communication). The latter fact has been shown to correlate with a displacement of the polar cap in a direction such as to increase the latitude of the polar cap-auroral boundary during morning hours (Heppner 1972).

Instrumentation

The payload included three magnetometers, namely a search coil with its axis perpendicular to the spin axis, a fluxgate magnetometer with its axis parallel to the spin axis and a dual-cell Cesium magnetometer; the payload also included two solar aspect systems. The search coil magnetometer sensor was an air core solenoid with a sensitivity of .67 microvolts·sec/gamma. The inflight signal, at the spin frequency of

approximately 6 Hertz, was amplified to two to three volts amplitude by a low noise amplifier with a voltage gain of 71.5. The fluxgate magnetometer consisted of a sensor with a range of $\pm$ 275 γ operated in a digitally controlled compensation field to extend its range to 60,000 γ (Ledley 1970). Calibration accuracy is estimated as .01% for the fluxgate and .1% for the search coil.

During the construction of the payload, fabrication methods and materials were chosen so as to reduce the magnitude of the magnetic field at the location of the magnetometer sensors. In addition, the sensors were located near the top of the nose cone; a minimum distance of half a meter existed between the magnetometer sensors and any other payload electronics. The magnetic field of the non-spinning payload at the location of the magnetometers was investigated by moving it up to a triaxial fluxgate magnetometer. This test was made in a magnetically quiet environment; it showed that the field due to the operating payload was less than 2γ. The induced eddy currents which would be generated in-flight by the spin of the vehicle in the ambient field were reduced by the use of a ceramic nose cone, a fiberglass skin for the payload and fiberglass deck plates.

The solar aspect system employed a novel application of a United Detector Technology silicon photodetector # SC 20. This device has independent electrical contacts to the four edges of its resistive substrate plus a connection to the photosensitive barrier junction on the other side of the diode. The ratio of the currents thru the four

substract contacts is a function of the distribution of light intensity across the face. By incorporating this device in a pin hole camera it can be used to determine solar aspect (U.S. Patent No. 3,744,913).

Data System and Payload Performance

Except for the Cesium magnetometer's signal, all the experiment signals were sent to an onboard 48 Khz PCM system, which included a twelve bit analog to digital converter. The main telemetry frame's commutator sampled twelve experiment signals (the eight photocell currents, one solar aspect system housekeeping word, the search coil voltage and the fluxgate analog and digital outputs) every 4 milliseconds. The PCM system's output signal was added to the Cesium magnetometers Larmor signal of approximately 200 Khz and the resulting signal was used to phase modulate the telemetry carrier. Data reception was generally good throughout the eight minute flight; near apogee, however, a significantly higher incidence of bit errors was observed and the Cesium signal to noise decreased to a level such that about 110 seconds of data were unprocessable. In addition, the Cesium magnetometer showed an intermittent malfunction for about thirty percent of the flight time. This consisted of a shift in frequency of 25γ when the instrument's heaters were on. The fluxgate, search coil and aspect system functioned normally throughout the flight.

Data Analysis

Modelling the motion of the payload: The payload was spin stabilized at approximately six revolutions per second. It precessed with a period of

40 seconds and a half cone angle of 1.5°. The equation of motion of a torque free rigid body, precessing without nutation, is used to describe the attitude of the payload. The determination of the parameters of the equation uses the measurements of the magnetic field and solar direction vectors. In the present description of the motion, the parameters are updated every forty seconds throughout the flight and linearly interpolated between the updates. Because of this it is not possible to describe variations in the field which have time constants comparable to, or longer than 40 seconds. Although the data clearly shows the existence of such field fluctuations the discussion is restricted to fluctuations with periods of a few seconds or less. (A description of the motion which will be valid at lower frequencies is being developed).

The measured magnetic field readings are filtered before use to obtain the parameters of motion. The fluxgate readings are numerically filtered with a 3 Hertz low pass filter. This removes the 6 Hertz modulation due to a 0.25° misalignment between the magnetometer and spin axes. A least squares fit of a sine wave was made to each cycle of the search coil voltage to obtain the direction and magnitude of the spin plane component of the field in payload coordinates. The filtering function of a least squares fit is not identical to the filter used on the fluxgate data, but no significant effects are noted in our final data due to this difference.

The sun direction in payload coordinates is obtained once or twice

per spin, the number, one or two depending on whether the sun crosses the field of view of one, or both sensors. Two measurements per spin were most common. The values of the elevation angle of the sun above the payload's spin plane are averaged to give one set of angles per spin. This set is then processed with a numerical low pass filter with a bandwidth of 0.075 Hertz. The solar azimuthal angle and the spin rate are determined by a sliding least squares fit of a quadratic function of time to phase angles from eighty successive measurements.

The parameters of motion are then derived as follows. The coning angle and the angle between the angular momentum vector $\vec{L}$ and the sun are obtained from the maxima and minima of the filtered solar elevation angle. The angle of $\vec{L}$ to the field is similarly determined from the field data. By using the field direction obtained from the field model, and the known solar direction, the vector $\vec{L}$ can be computed in a known coordinate system.

The two parameters, precessional angular velocity and phase, are then obtained from the solar elevation data; the solar elevation angle is described by the model of motion with the two parameters above as unknown variables, which are then computed by substitution of the measured solar elevation data. The parameters of motion are shown in Table 1 as a function of time from launch.

Results

Figure 2 shows the measurements after their transformation into a non-precessing coordinate system. It is a plot, in topographic cartesian

coordinates, of the three components of the vector difference of the measured field minus the field model for the 18.128 flight. The X trace is displaced upward and Z downward by one hundred gammas to reduce overlap. The X, Y and Z axes in topographic coordinates have the directions of geographic North, East and down, respectively. The Z axis makes an angle of only 3° with the ambient magnetic field. Figure 3 shows the same quantities plotted for the 18.129 flight, which took place in relatively undisturbed fields. It is included here to illustrate the noise level of the measurement and analysis technique. The small, rapid noise fluctuations in the 18.129 data with periods of less than five seconds are larger in the X and Y directions than in the Z direction. This is due to the fact that the largest source of noise in the measurements is in the determination of the phase angle of the field in payload coordinates. This noise contributes mostly to the X and Y topographic components. There are also larger variations in the 18.129 data with a period of 40 seconds (the precession period) due to inadequacies in the description of motion. The wide excursions at the beginning and end of the flight are due to changes in the attitude of the payload caused by atmospheric drag.

It is clear from Figure 2 by comparing the X and Y plots with the Z plot that transverse field fluctuations of the order of a hundred gammas with periods ranging from one or two seconds up to several tens of seconds were detected in the 18.128 flight, although as explained above, the description of motion will not give an accurate representation

of the longer period fluctuations.

Power spectra were computed from these data. Figure 4 shows the spectral density for the Y topographic component for the first half (100 seconds to 250 seconds) of each flight. The power spectral density for the 18.128 flight at all frequencies between 0.2 and 0.7 Hertz is more than an order of magnitude greater than that for the 18.129 flight. In addition, the 18.128 spectrum has a statistically significant peak centered at about 0.42 Hertz, which is absent from the 18.129 spectrum. The power spectrum for the second half of the 18.128 flight was also computed. It has power levels between 0.2 and 0.7 Hertz which are about one half of those from the first half of the flight, and there is not a statistically significant peak. The levels are still significantly above those of the 18.129 flight in that frequency range.

The only frequency region in which the power spectral density for 18.129 exceeds that of 18.128 is above 2 Hertz. However, preflight measurements had shown that the solar sensors used in the 18.129 flight had a higher noise level than those used in the 18.128 flight, and this, rather than field fluctuations may be the cause of the higher 18.129 spectral density above 2 Hertz.

A more accurate estimate of orthogonality to the ambient field may be obtained during individual large fluctuations by examining the variation of the difference of the measured field magnitude minus the model field magnitude. Individual fluctuations are shown more clearly

in Figure 5 which is an expansion of Figure 2 between 100 and 150 seconds. The scalar field was examined between 123.75 and 125.25 seconds when a relatively isolated fluctuation occurs in the difference vector. The field magnitude was calculated from the vector magnetometers in order to avoid the offset problems mentioned earlier with the Cesium magnetometer. The field magnitude differences during this fluctuation were averaged and compared with the average during the one second preceding and following the fluctuation. The difference was 0.2γ; the corresponding difference in the vector field was 55γ. This is consistent with a fluctuation which is at 89.8° to the ambient field.

Two possible models for these fluctuations were considered, namely: (1) that they were transverse plane hydromagnetic waves with a horizontal wavefront of dimensions at least as large as the flight path, i.e. 200 km, or, (2) that they were caused by the payload's motion through quasi-stationary field aligned currents. The latter is the model adopted by previous workers to explain their polar cusp observations made at higher altitudes. It is also the model used to explain nightside observations at both satellite and sounding rocket altitudes (Park and Cloutier 1971). It appears that the latter model is also required for our observations. Triaxial fluxgate magnetometers were operated on the ground at Hall Beach and CAM-4, which is 250 kilometers west of Hall Beach. These instruments have a noise level of $\sim 1\gamma$ and a bandwidth of 50 Hertz. Each axis was sampled once every three seconds for chart recording. No noise or aliased fluctuations above the 1γ level were

recorded during the 18.128 flight. Calculations of the attenuation of transverse hydromagnetic waves, in propagating through the lower ionosphere to the ground, yield attenuation factors of from 4 to 20 in the frequency range of these observations (Greifinger 1972). Effects of the fluctuations should therefore have been detectable on the ground if they had been hydromagnetic waves.

If it is assumed that fluctuations are due primarily to the payload's motion through a current system, then it is possible to model some of the individual current forms. The 1.5 second fluctuation centered at 124.5 seconds can again be used as an example. If a base line is established through the fluctuation by linearly interpolating the average values for the one second preceding and following the event, a fluctuation is obtained which has a peak value of 100γ in X and 64γ in Y. The X and Y components rise and fall approximately (a) linearly and (b) with a rise time which is the same as the fall time. A field signature such as this can be generated by two adjacent constant density current sheets of opposite signs. The direction of the normal to the plane of the sheets would have a geographic azimuth of 305° with the downward current sheet being the south-easterly one of the pair. The measured magnetic North has a geographic azimuth of approximately 310°, so these current sheets are aligned along the local magnetic East-West direction.

The horizontal thickness computed for the sheets depends upon the assumption made about their velocity. If it is assumed that they are stationary, the thickness of each sheet is ~ 330 meters. The current

density is then 2.9×10^{-4} amps/m^2. This thickness is a normal one for auroral structures; for example Maggs and Davis (1968) found a median thickness of 230 meters for a set of 581 auroral structures. On the other hand, the calculated current intensity of 2.9×10^{-4} amp/m^2 is higher than any previously reported. Walen and McDiarmid (1972) reported the measurement of precipitating electron fluxes in auroral arcs which they conservatively estimate to correspond to currents of 2×10^{-4} amp/m^2. However, their measurements were made at a local time of 2030, well removed from the dayside polar cusp region. In the cusp region current densities of $\leq 10^{-5}$ amp/m^2 are commonly reported; the maximum density, of 9×10^{-5} amp/m^2 was reported by Zmuda and coworkers (Armstrong 1973).

If it is assumed that the current sheets were convecting, a reasonable maximum value for their velocity normal to their plane (i.e in the direction of the payload's horizontal velocity) would be 2 km/sec, based on the 18.127 sounding rocket electric field measurements of Maynard and Johnstone (1973), which were made at nearly the same local time. The current sheets would then be overtaking the payload with a relative velocity of 1.5 km/sec. A thickness for each sheet of one kilometer is obtained, and a current density of 9×10^{-5} amp/m^2. This current density is still at the maximum of all earlier observations. However, the present magnetic field measurements have higher temporal and spatial resolution which permits detection of smaller, and apparently more intense structures than before.

Maynard and Johnstone (1973) observed several bursts of soft precipitating electrons in one of their flights made during this expedition. A comparison of current density estimates from this paper with their particle flux intensities is possible if it is assumed that the upward current sheet is caused by precipitating electrons with the same velocity distribution derived by Maynard and Johnstone. This is a Maxwellian velocity distribution with a temperature of 1.2×10^6 ^oK. Assuming an isotropic angular distribution in the downward hemisphere, a density of 43 electrons cm^{-3} is obtained which is similar to the maximum calculated during bursts by Maynard and Johnstone. This high electron energy density observed at 195 km supports suggestions that electron energization mechanisms exist in the lower cusp region.

Finally, it should be noted that only one well resolved fluctuation has been selected for analysis. Inspection of Figure 5 clearly shows that there are possibilities for a wide variety of current forms in this region.

Conclusions

(1) A sounding rocket measurement of magnetic fields in the polar cusp ionosphere with a measurement resolution of approximately 100 meters along the ground detected a more or less continuous, intense, fine structured field aligned current system throughout the entire 150 kilometer magnetic North-South path of the flight.

(2) The power spectra of the field fluctuations indicates a preferred dimension of $\sim$ one kilometer or less for the current system

Acknowledgements

The authors gratefully acknowledge the dedicated engineering support provided by W. C. Folz and S. W. Billingsley and the assistance in data reduction provided by M. Miller.

REFERENCES

Armstrong, J. C., Field-aligned currents in the magnetosphere, presented at the Summer Advanced Institute, "Earth Particles and Fields", 1973 (to be published).

Berko, F. W., R. A. Hoffman, R. K. Burton and R. E. Holzer, Simultaneous particle and field observations of field-aligned currents, (Submitted to J. Geophys. Res.).

Burch, J. L., Low-energy electron fluxes at latitudes above the auroral zone, J. Geophys. Res., 73, 3585, 1968.

Cahill, L. J., Jr., Detection of an electric current in the ionosphere above Greenland, J. Geophys. Res., 64, 1377, 1959.

Choy, Lawrence W., R. L. Arnoldy, W. Potter, P. Kintner, and L. J. Cahill , Jr., Field-aligned currents near an auroral arc, J. Geophys. Res., 76, 8279, 1971.

Fairfield, D. H., and N. F. Ness, Imp 5 Magnetic-field measurements in the high-latitude outer magnetosphere near the noon meridian, J. Geophys. Res., 77, 611, 1972.

Frank, L. A., Plasma in the earth's polar magnetosphere, J. Geophys. Res., 76, 5202, 1971.

Greifinger, Phyllis, Ionospheric propagation of oblique hydromagnetic plane waves at micropulsation frequencies, J. Geophys. Res., 77, 2377, 1972.

Gurnett, D. A., Satellite measurements of DC electric fields in the ionosphere, Particles and Fields in the Magnetosphere, (ed) B. M. McCormac, D. Reidel Publishing Co., Dordrecht, Holland, p. 239, 1970.

Heikkila, W. J., and J. D. Winningham, Penetration of magnetosheath plasma to low altitudes through the dayside magnetospheric cusps, J. Geophys. Res., 76, 883, 1971.

Heikkila, W. J., J. D. Winningham, R. H. Eather and S.-I. Akasofu, Auroral emissions and particle precipitation in the noon sector, J. Geophys. Res., 77, 4100, 1972.

Heppner, J. P., Magnetospheric convection patterns inferred from high latitude activity, Atmospheric Emissions (ed. B. M. McCormac and A. Omholt), Van Nostrang Reinhold Publishing Co., N.Y., p. 251, 1969.

Heppner, J. P., Polar-cap electric field distributions related to the interplanetary magnetic field direction, J. Geophys. Res., 77, 4877, 1972.

Hoffman, R. A., Low-energy electron precipitation at high latitudes, J. Geophys. Res., 74, 2425, 1969.

Langel, R. A., Near earth magnetic disturbance in total field at high latitudes, GSFC Report X-645-73-225, 1973 (submitted to J. Geophys. Res.).

Ledley, B. G., Magnetometers for space measurements over a wide range of field intensities, Rev. de Phys. Appliquée., 5, 164, 1970.

Maggs, J. E., and T. N. Davis, Measurements of the thicknesses of auroral structures, Planet. Space Sci., 16, 205, 1968.

Maynard, N. C., and J. P. Heppner, Variations in electric fields from polar orbiting satellites, Particles and Fields in the Magnetosphere, (ed) B. M. McCormac, D. Riedel Publishing Co., Dordrecht, Holland, p. 274, 1970.

Maynard, N. C., and A. D. Johnstone, High-latitude dayside electric field and particle measurements, J. Geophys. Res., (to be published).

Park, R. J., and P. A. Cloutier, Rocket-based measurement of Birkeland currents related to an auroral arc and electrojet, J. Geophys. Res., 76, 7714, 1971.

Piddington, J. H., The magnetosphere and its environs, Planet. Space Sci. 13, 363, 1965.

Russell, C. T., C. R. Chappell, M. D. Montgomery, M. Neugebauer and F. L. Scarf, Ogo 5 observations of the polar cusp on November 1, 1968, J. Geophys. Res., 76, 6743, 1971.

Sharp, R. D., and R. G. Johnson, Satellite measurements of auroral particle precipitation, Earth's Particles and Fields, (ed.) B. M. McCormac, Reinhold Book Corporation, New York, p. 113, 1968.

Whalen, B. A., and I. B. McDiarmid, Observations of magnetic-field-aligned auroral-electron precipitation J. Geophys. Res., 77, 191, 1972.

Zmuda, A. J., J. H. Martin and F. T. Heuring, Transverse magnetic disturbances at 1100 kilometers in the auroral region, J. Geophys. Res., 71, 5033, 1966.

Zmuda, A. J., J. C. Armstrong, and F. T. Heuring, Characteristics of transverse magnetic disturbances observed at 1100 kilometers in the auroral oval, J. Geophys. Res., 75, 4757, 1970.

TABLE 1: PARAMETERS OF MOTION

T (sec)	θ_L (deg.)	ϕ_L (deg.)	θ_p (deg.)
80	79.314	23.11	1.585
120	79.332	23.13	1.587
160	79.350	23.19	1.595
200	79.357	23.26	1.600
240	79.357	23.30	1.603
280	79.354	23.40	1.601
320	79.351	23.57	1.591
360	79.344	23.75	1.594
400	79.336	23.96	1.601
440	79.336	23.96	1.601

θ_L and ϕ_L are the spherical coordinates of the angular momentum vector, $\vec{L}$. θp is the half cone angle. The angular frequency of the precessional motion was kept constant at 8.870 degrees/sec. The phase of the precessional motion was defined by a minimum in the solar elevation angle at 82.43 seconds.

FIGURE TITLES

Figure 1. The magnetic disturbance vectors during the 18.128 flight at 1650 UT on March 22, 1971. The vertical disturbance component in gammas (1 gamma = 1 nanotesla) is shown by the number beside each station location. An upward disturbance is negative.

Figure 2. The components of the vector difference field (measured minus model) for the 18.128 flight in topographic cartesian coordinates. The X and Z traces are displaced by $\pm$ 100 gammas respectively, to reduce overlap.

Figure 3. The components of the vector difference for the 18.129 flight.

Figure 4. Power spectra of Y topographic difference components. A dot symbol is used for the 18.128 spectrum and an X symbol for 18.129.

Figure 5. A time expanded plot of Figure 2, showing the rapid field fluctuations observed during the 18.128 flight from 100 to 150 seconds.

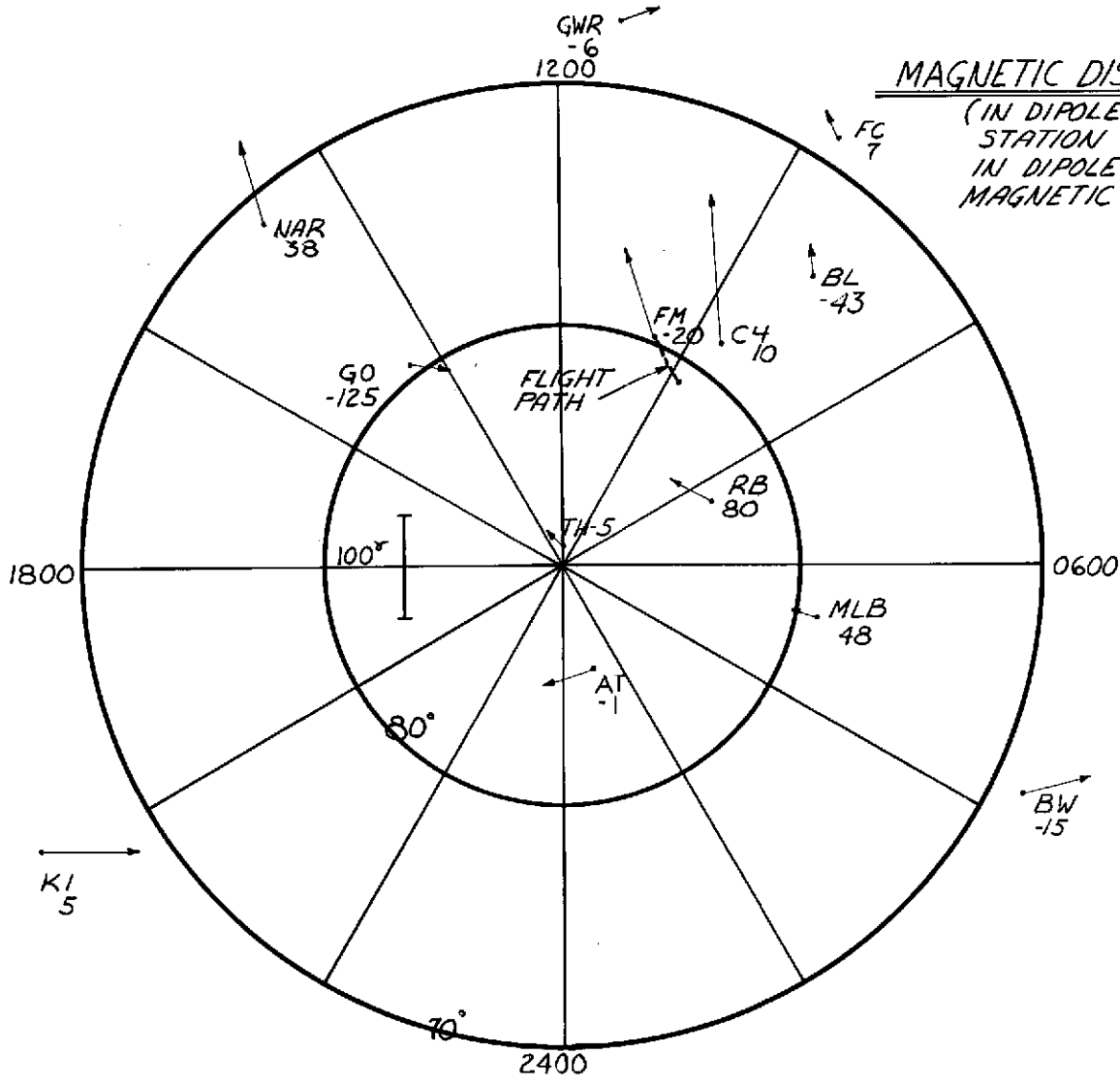

MAGNETIC DISTURBANCE VECTORS

(IN DIPOLE COORDINATES)
STATION LOCATIONS ARE PLOTTED
IN DIPOLE LATITUDE AND
MAGNETIC TIME COORDINATES

STATIONS

AT	ALERT
BL	BAKER LAKE
BW	BARROW
C4	CAM 4
FC	FORT CHURCHILL
FM	FOX MAIN
GO	GODHAVEN
GWR	GREAT WHALE RIVER
KI	KIRUNA
MLB	MOULD BAY
NAR	NARSSARSSUAQ
RB	RESOLUTE BAY
TH	THULE

FIGURE 1

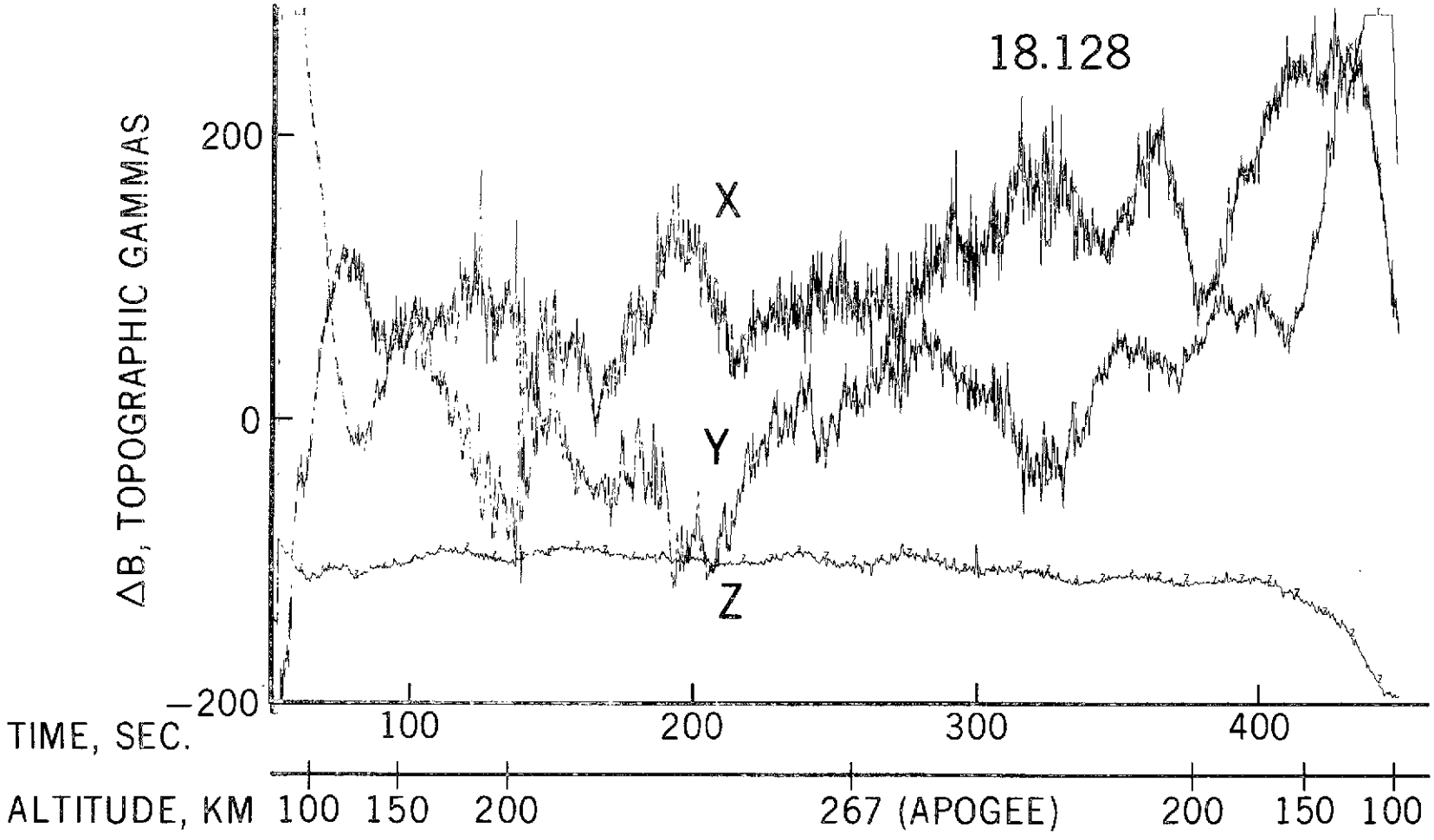
18.128
ΔB, TOPOGRAPHIC GAMMAS
200
0
−200
X
Y
Z
TIME, SEC.
100
200
300
400
ALTITUDE, KM 100 150 200 267 (APOGEE) 200 150 100

FIGURE 2

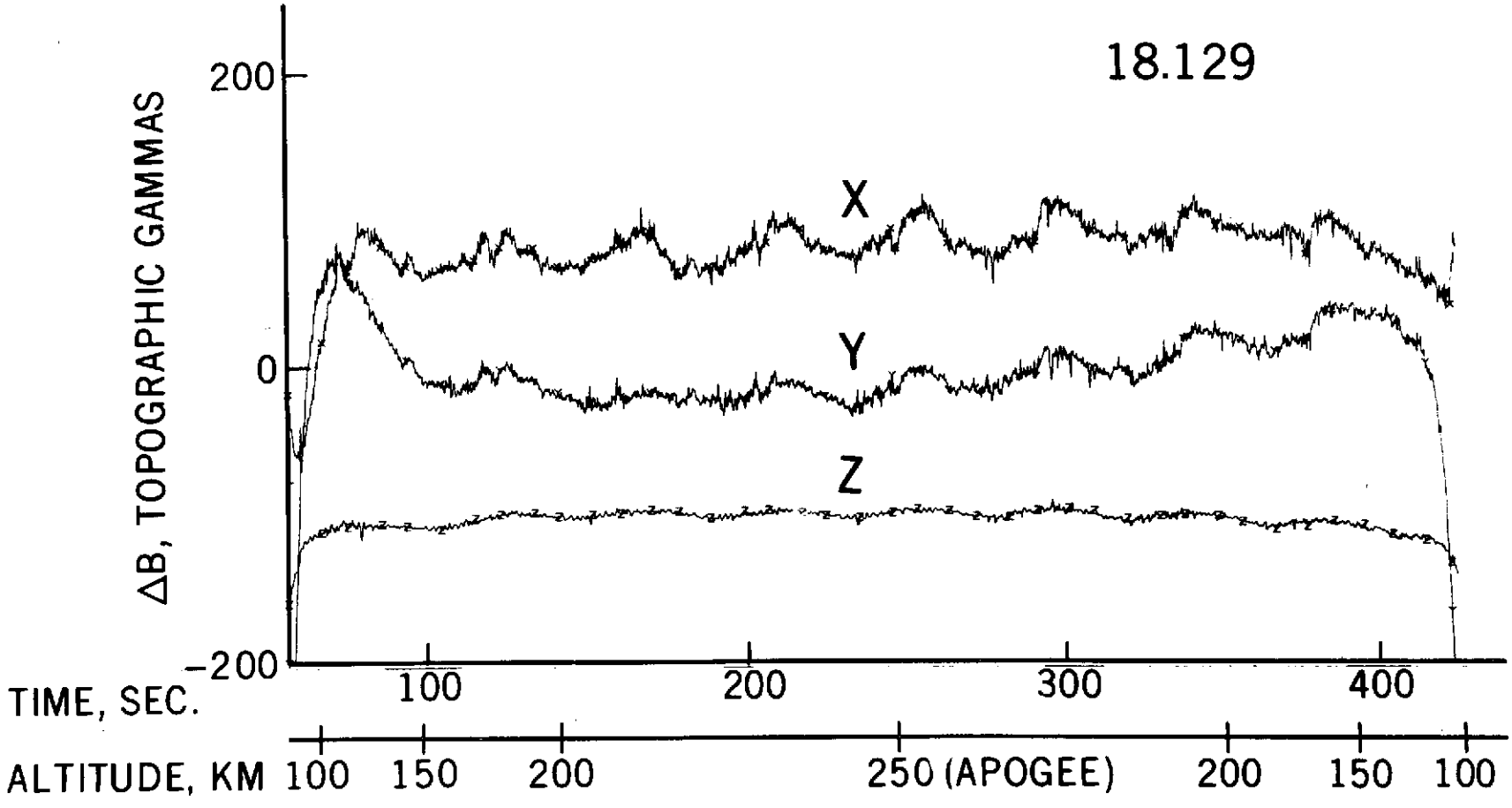
18.129
200
0
−200
ΔB, TOPOGRAPHIC GAMMAS
X
Y
Z
100
200
300
400
TIME, SEC.
ALTITUDE, KM 100 150 200 250 (APOGEE) 200 150 100

FIGURE 3

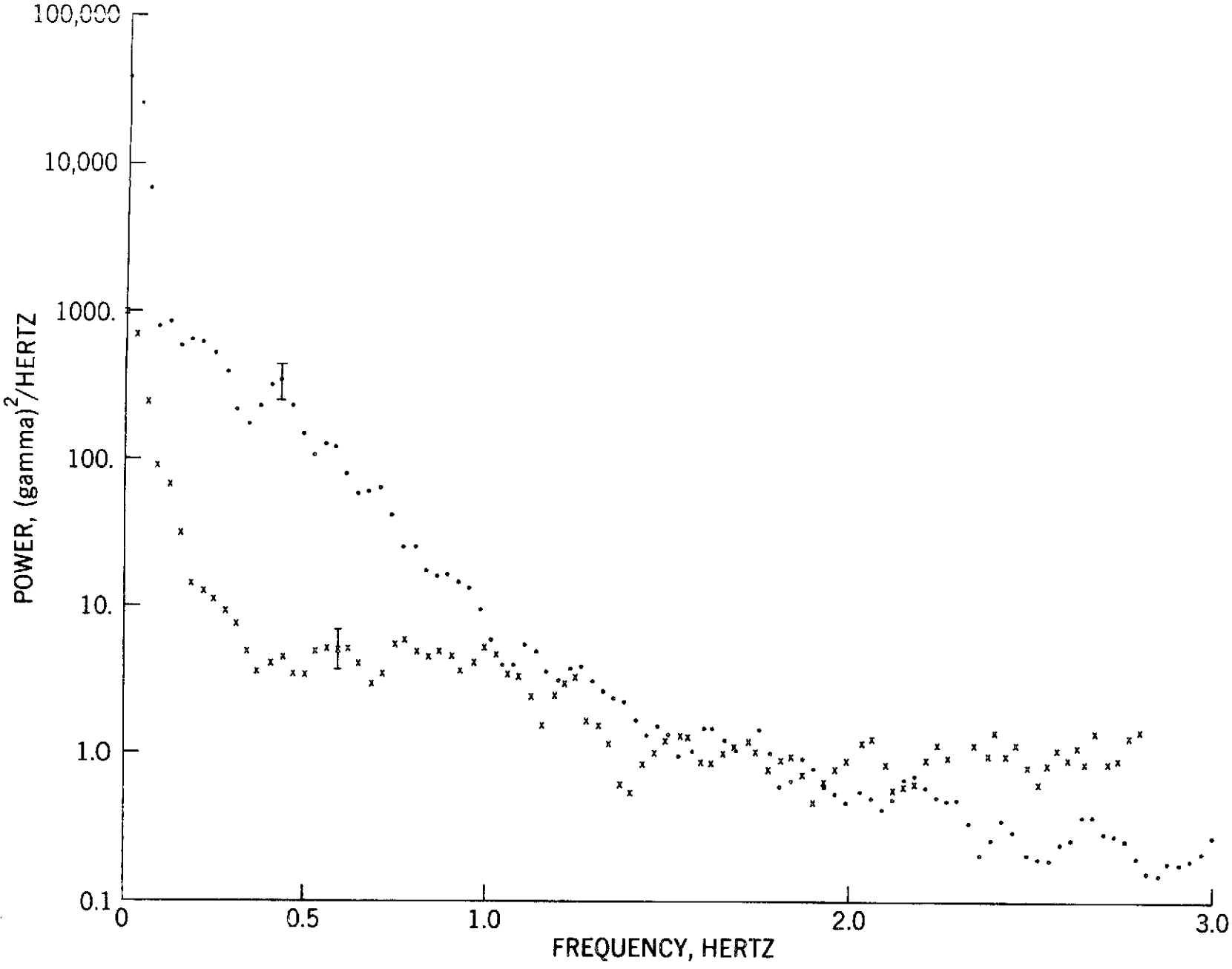
100,000
10,000
1000.
100.
10.
1.0
0.1
POWER, (gamma)^2/HERTZ
0
0.5
1.0
2.0
3.0
FREQUENCY, HERTZ

FIGURE 4

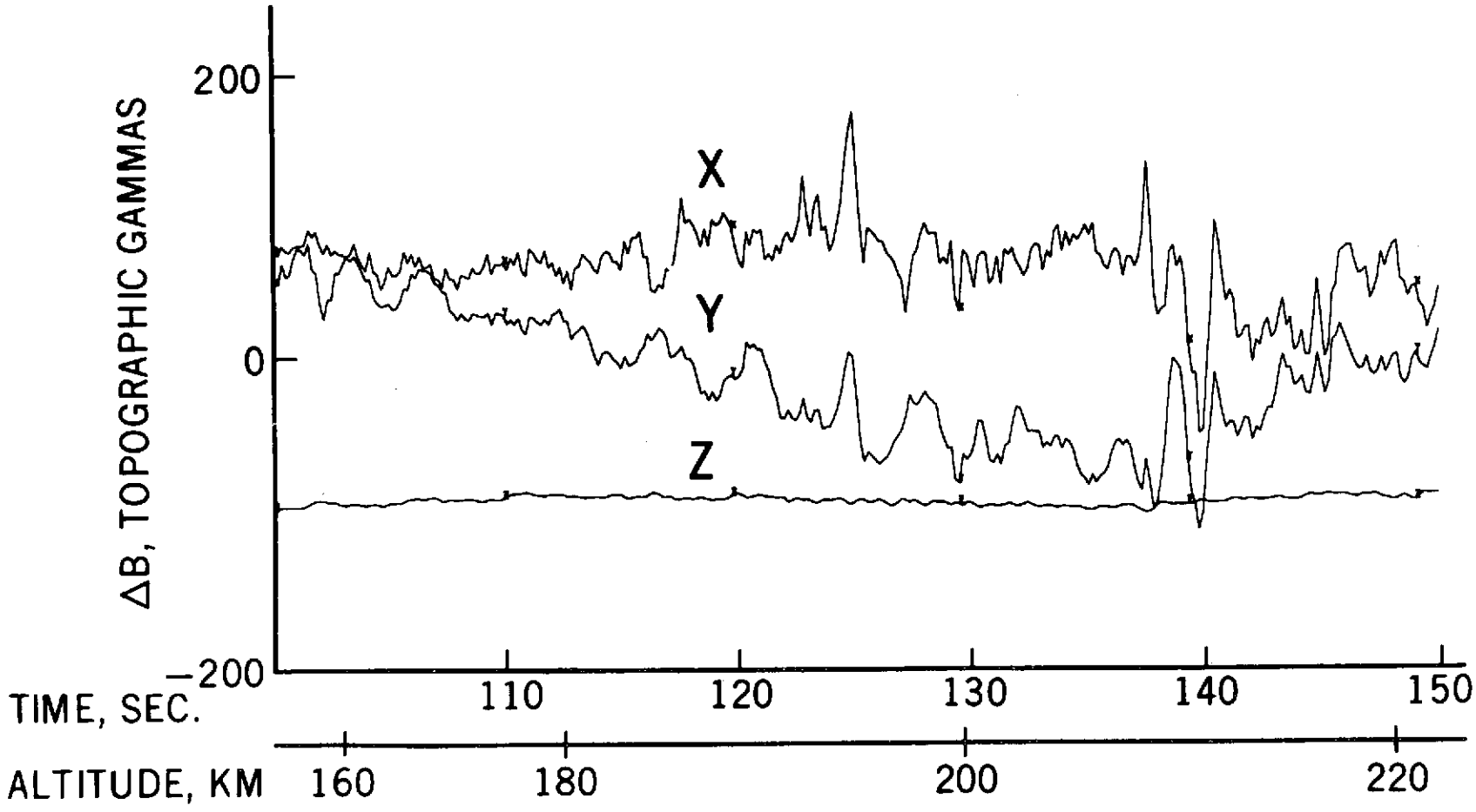

FIGURE 5

NASA—GSFC